

Advanced Aerosol Separator for PM_{2.5} Chemical Composition and Size Distribution Analysis

David Keicher¹, Marcelino Essien², Fa-Gung Fan³

Integrated Deposition Solutions (IDS), Inc., 5901 Indian School Rd NE Suite 125, Albuquerque, NM 87110

Nicolas Verdier⁴

Centre National d'Etudes Spatiales (CNES), 18 Avenue Edouard Belin, 31401 Toulouse CEDEX 9, France

Jean-Baptiste Renard⁵

LPC2E-CNRS, 3A avenue de la recherche scientifique, 45071 Orléans cedex 2, France

Jurij Simcic⁶ and Dragan Nikolić⁷

Jet Propulsion Laboratory (JPL), California Institute of Technology, 4800 Oak Grove Drive, Pasadena, CA, 91109

We report on progress made in the design of compact NanoJet Flow Cell (NJFC), its operational stability and integration with both the JPL Micro-Electro-Mechanical Systems (MEMS) Piezoelectric Valve (PV) and the vacuum-compatible Light Optical Aerosol Counter and Sizer (LOAC). The apparatus will be differentially pumped and attached to a 3D printed non-corrosive vacuum chamber for Residual Gas Analysis (RGA). The aerosol separator will be used in real-time monitoring of aerosol particles in the ambient air at a wide range of pressures, by optically determining their refractory nature (solid vs. liquid, spherical vs. complex morphology) and size distribution. When vaporized on the RGA's hot filament, aerosol particles can be analyzed for their chemical composition using Mass Spectrometry (MS) methods. Cyclone separator will be used to recycle the carrier (sheath) gas and examine the aerosol separator susceptibility to clogging as a function of the purity of the sheath gas. Optimal gas flow rates and operational parameters will be tuned to provide the highest possible transmissions for PM_{2.5} aerosols detrimental to the human respiratory system.

Nomenclature

AS	= Aerosol Separator	QIT-MS	= quadrupole ion trap mass spectrometer
PM _{2.5}	= Particulate Matter <2.5µm in size	TRL	= technology readiness level
µm	= micrometer	SRS	= Stanford Research Systems
IDS	= Integrated Deposition Solutions	DPS	= differentially pumped vacuum system
CNES	= Centre National d'Etudes Spatiales	mTMP	= miniature turbo-molecular pump
JPL	= Jet Propulsion Laboratory	mSP	= miniature scroll pump
NJFC	= NanoJet flow cell	DMA	= differential mobility analyzer
MEMS	= micro-electro-mechanical systems	VOAG	= vibrating orifice aerosol generator
PV	= piezoelectric valve	SEMS	= scanning electrical mobility spectrometer
LOAC	= light optical aerosol counter	SMPS	= scanning mobility particle sizer
RGA	= residual gas analysis	CPC	= condensation particle counter
MS	= mass spectrometer		

¹CEO and Vice President, IDS Inc.

²CSO and President, IDS Inc.

³Consultant, IDS Inc.

⁴Engineer, DCT/BL/NB.

⁵Senior Scientist, LOAC instrument

⁶Technologist, 389T - Planetary Mass Spectrometry, Mail Stop: 306-392.

⁷Technologist, 389T - Planetary Mass Spectrometry, Mail Stop: 306-392.

I. Introduction

WE report on the design of an Aerosol Separator (AS) as the gaseous sample inlet for any mass spectrometer operating in an atmosphere containing suspended aerosols, including liquid, icy and metallic particles. This compact apparatus will be used to study long-term variations in composition, number, and size of aerosols by inertially separating them from the gas phase using the Nanojet Flow Cell¹ (NJFC) technology shown in Fig. 1. The apparatus will tolerate changes in atmospheric pressure of up to three orders of magnitude while performing high-yield segregation of aerosols from the dominant gas phase. When attached to a mass spectrometer, it will enable *in situ* real-time studies of the chemical composition of aerosols at parts-per-billion sensitivity and 20 full mass spectra per second^{2,3}. When coupled to the Light Optical Aerosol Counter⁴ (LOAC) sensor, it will measure number density, refractory properties, and size distribution of aerosols. Instrumentation for aerosol mass spectrometry is a well-established field both in industry and academia⁵. However, these are not well suited for planetary missions due to mass and size and because they operate in a narrow range of outside pressures. Here, we remove these limitations by devising an ultra-compact AS capable of tolerating broad changes in external pressure while handling a variety of aerosols. The target mass/volume factor for the entire system is under 2kg/2L with four miniature Creare pumps excluding the LOAC sizer⁴ and their supporting electronics.

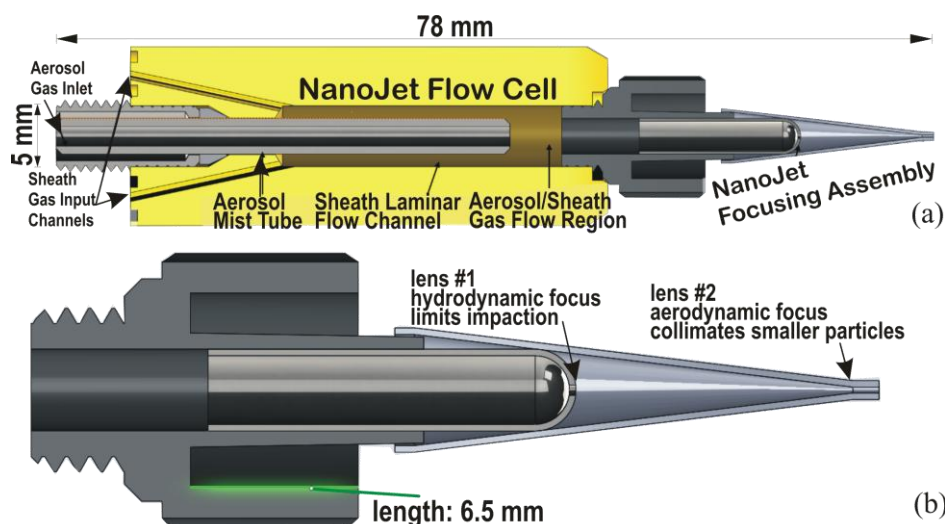


Figure 1: The NanoJet Flow Cell. A cross-sectional view of the NanoJet Flow Cell (a) labeled with a role/function for each feature and compact design of the NanoJet focusing assembly (b).

An overview of the complete apparatus is given in Fig. 2, which we will use, as a challenging case, to investigate an AS appropriate for analyzing the corrosive/metallic type of aerosols. Corrosive aerosols are irritants and cause tissue damage, wherever they make contact with the respiratory tract. In Figure 2, the AS can be attached to any mass spectrometer, for example, the JPL quadrupole ion trap mass spectrometer^{2,3} (QIT-MS, at TRL-6). Presently the QIT-MS would need to be modified to perform aerosol vaporization on one of its electrodes. Instead, as a proof of principle, we will use a 200-amu RGA sensor from the Stanford Research Systems (SRS). RGA's hot filament acts as the aerosol vaporizer and gas ionizer for the RGA's quadrupole mass filter. The AS set-up is shown in Fig. 2, will enable new science by extending any mass spectrometer's capabilities to perform compositional analysis of aerosols.

The AS has three components, as shown in Fig. 2: (a) an *adjustable piezoelectric aperture* (TRL-4, developed by JPL); (b) an *aerodynamic lens* (TRL-2, based on the NJFC⁶ technology) developed by the Integrated Deposition Solutions, Inc. (IDS); (c) a *differentially pumped vacuum system* (DPS), to be designed by IDS and JPL to support future inclusion⁷ of miniature Creare turbo-molecular pumps (mTMP, 0.13kg) and scroll pump⁸ (mSP, 0.33kg). Both types of Creare pumps were used on Mars in the SAM⁹ and MOMA¹⁰ instruments, and their performance in this study is modeled by a single laboratory-sized turbo molecular pump (Pfeiffer HiCube 80 Eco pump). As shown in Fig. 2, the HiCube 80 pump is attached to two separate DPS pump ports with a gas line manifold. The manifold has a different conductance in each gas line and provides equivalent pumping speeds on each pump port as if miniature Creare pumps were used.

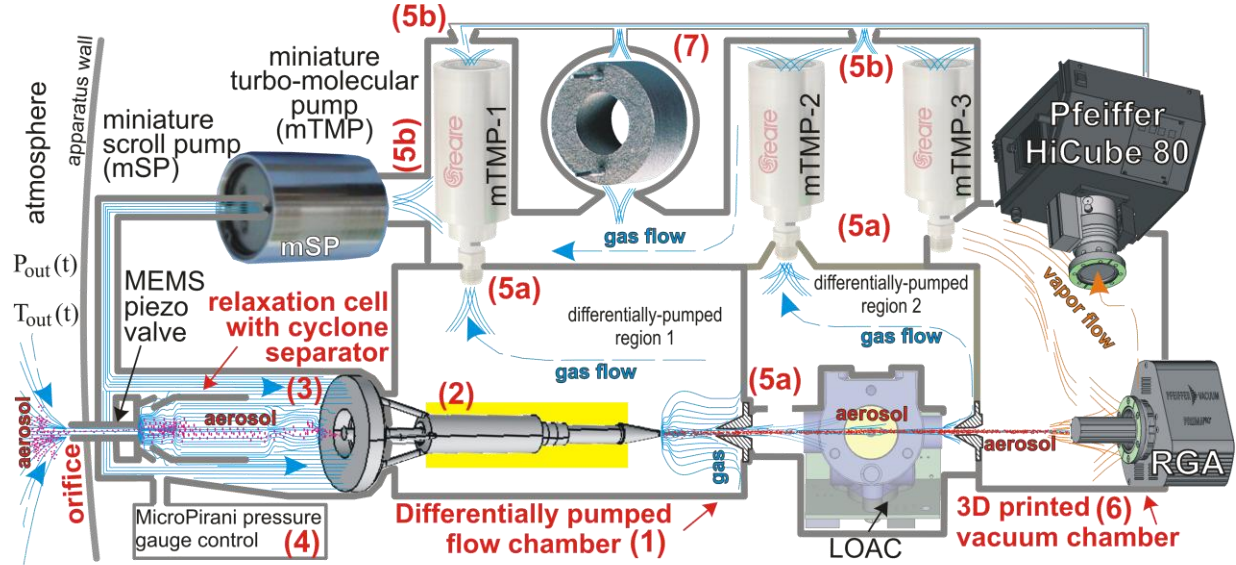


Figure 2: Block diagram of the test set-up. The AS apparatus is placed inside a differentially pumped flow chamber (1) designed as a sample inlet to any mass spectrometer. Blue color streamlines represent the atmosphere gas flow, whereas red dots are suspended aerosol particles. This study aims to advance to TRL4 all of the components marked in red ink: the NanoJet Flow Cell (2), relaxation cell with the cyclone separator (3), micropirani pressure gauge (4), internal (5a) and external (5b) vacuum ports, and non-corrosive 3D-printed vacuum chamber (6). The readily available components are: the JPL MEMS valve; a mobile Pfeiffer HiCube 80L/s Eco pump system as a replacement for Creare pumps, and the 200-amu RGA from the Stanford Research Systems (SRS) used as the mass detector and as the aerosol vaporizer. A leak-tight LOAC optical particle counter/sizer is an optional module currently being built under JPL/CNES collaboration. It can be attached on-demand, like the St172 sintered porous getter (7), which serves as a static gas sink.

The MKS 905 MicroPirani¹¹ is a calibrated vacuum pressure transducer. Its MEMS-based pressure sensor is mounted on Klein Flansche 16 flange for easy vacuum integration and includes a measuring electronics module connected to the PDR900 single-channel controller via the TTL UART interface. The digital interface on the controller transfers real-time data directly to a host processor, which we use to monitor and regulate the gas flow through the MEMS piezoelectric valve.

Traditional cyclone separators use the centrifugal acceleration of aerosols with different sizes ($>5 \mu\text{m}$) and densities larger than the carrier gas to mechanically separate and collect particles in an outer vortex flow. In contrast, particle-free gas is extracted through an inner vortex flow. Small cyclone separators ($<5 \text{ cm}$) with high collection efficiencies¹² are used as bioaerosol samplers in air quality control units in clean rooms and hospitals. Here we use a cyclone to process the sheath gas and remove particles (wet or dry) from the sheath gas to ensure that the sheath gas that provides a gas buffer layer between the atmospheric particles and the aerodynamic lenses is particle free. Particle in the sheath gas would degrade the particle separator's performance and lead to clogging of the particle sampling system in long operations.

II. Adjustable Piezoelectric Aperture

A prerequisite for any airborne aerosol inlet is that the performance of its aerodynamic lens is *not affected* by changes in atmospheric pressure, $P_{\text{out}}(t)$, and temperature, $T_{\text{out}}(t)$. The performance of the proposed aerodynamic lens is modeled against 18 to 760 Torr variations in the atmospheric pressure, P_{out} , and 220K to 340K changes in atmospheric temperature T_{out} . If an atmosphere sample is admitted into the relaxation cell via the circular orifice of fixed diameter d_f , the pressure in the relaxation cell $P_{\text{rx}}(t)$ will change proportionally to $P_{\text{out}}(t)$. This change will affect the performance of any aerodynamic lens if it is designed to work at constant inlet pressure. Hence, the need for an adaptive inlet aperture which can be contracted or expanded as required (see Fig. 3). The range for the effective diameter, d_f , that will maintain near-constant pressure in the relaxation cell, is 100 to 550 μm . At 760 Torr atmosphere pressure, the amount of admitted gas through a single orifice of 550 μm in diameter will saturate the DPS and incapacitate the mass spectrometer.

Moreover, much-needed regulation of gas sample intake cannot be provided by several smaller apertures operated in parallel due to the operational complexities of their state control. Versatile fixed-aperture piezoelectric systems with linear strokes up to 700 μm do exist¹³ but require from -20 V to 130 V to operate. These are exclusively used as injectors of collimated thermal gas beams into fusion vacuum chambers and susceptible to blockage by particles present in the fuel gas.

To handle the extensive range of input pressures, we limit the atmosphere sample flow using the JPL Micro-Electro-Mechanical Systems (MEMS) piezoelectric valve¹⁴ (see Fig. 3a), which requires no further development¹⁵. The gap, G , between the boss and the valve seat is increased by applying 0-65 Vdc to the piezoelectric stack, which provides low power (mW) control of the flow rate into the valve outlet. When fully closed at 0 Vdc, the piezoelectric valve can withstand outside pressures of up to 60 bar. By continuously adjusting the gap G size, we sustain a constant pressure, $P_{\text{rlx}}=2.1$ Torr, in the relaxation cell despite changes in the atmospheric pressure, $P_{\text{out}}(t)$, and maintain the performance of the aerodynamic lens. Figure 3d shows a concentric seat rings over which the cascading gas flow is established. In Fig. 3c aerosol particles are entrenched in the gas streamlines and carried through the gap, G , above the seat ring. Using the LOAC counter and sizer, we will measure the particle transmission efficiency through the piezoelectric valve as a function of particle size for the range of operating pressures.

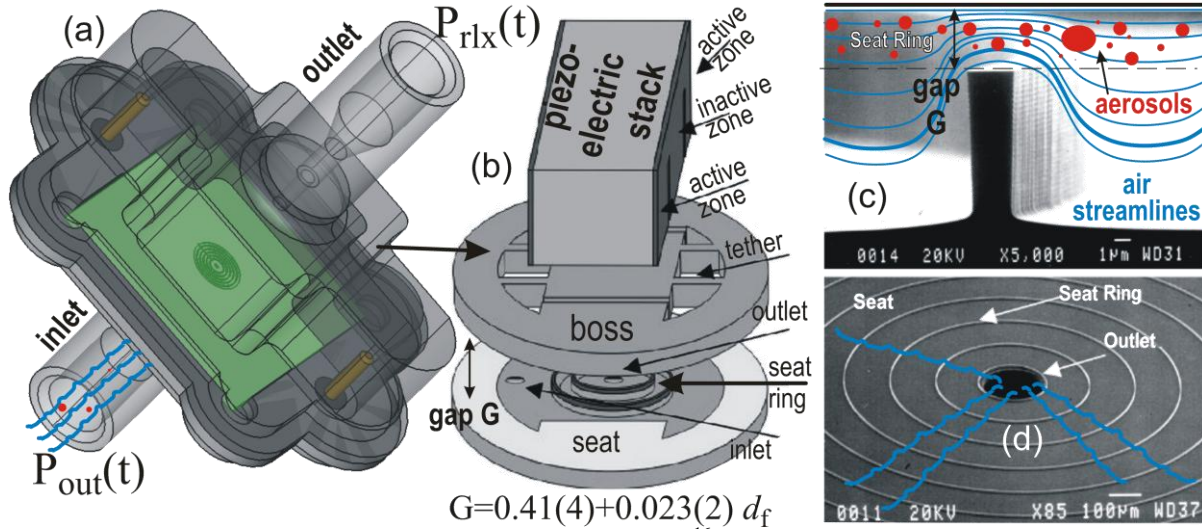


Figure 3: JPL MEMS piezoelectric valve. (a) ANSYS Fluent¹⁶ model used to simulate compressible airflow through piezoelectric valve¹⁴; (b) piezoelectric stack lifts the boss membrane placed on top of ten concentric (9 μm tall, 3 μm wide) seat rings (c) creating a gap, G , and regulates the gas flow into the outlet ((d), 250 μm wide); summary of modeling results (in μm) is a linear relationship between the piezo valve gap, G , and its equivalent diameter, d_f , for which the outlet pressure P_{rlx} remains at 2.1 Torr.

The ANSYS Fluent¹⁶ model of the valve seat is illustrated in Fig. 3a. The gas inlet is held at different pressures $P_{\text{out}}(t)$, temperatures $T_{\text{out}}(t)$, and the gas outlet is always kept at the constant pressure $P_{\text{rlx}} = 2.1$ Torr set by the pumping capacity of miniature Creare pumps and conductance of differentially-pumped system. The valve seat, seat rings, and gas outlet were kept at room temperature. Then we vary the gap size, G , and compute the compressible pV flow rate through the piezoelectric valve using pressure and temperature-dependent viscosity of the gas. This flow rate is then matched to the flow rate provided by a single circular inlet aperture of the diameter, d_f . Figure 3 summarizes modeling results in the form of a linear relation between the piezo valve gap, G , and the effective diameter, d_f , for which the admitted gas flow will sustain $P_{\text{rlx}} = 2.1$ Torr at the inlet of the aerodynamic lens. Circular orifice plates with effective diameter, d_f , are easily fabricated and will be used as inlet apertures for testing differential pumping system before integration of aerodynamic lens and piezoelectric valve. The loss of aerosols on the seat rings of the current MEMS piezoelectric valve design is expected for particles larger than 7 μm , but future models will target 12 μm size cut-off.

III. Aerodynamic Lens

The aerodynamic lens shown in Figs. 2 and 4 is based on the proprietary IDS ultra-compact NanoJet technology⁶. Furthermore, our previous modeling results^{17, 18, 19, 20} confirm that particles of varying size suspended in the gas can be separated from the gas phase and jetted into the vacuum chamber containing getter pump and the mass spectrometer at chamber pressures $P_{\text{chm}} < 1\text{E-}9$ Torr. Initial experimental results are encouraging and support the modeling efforts.

A. Preliminary Modeling

In Fig. 4 we present simulation results that show optimal flow rates for both the sheath gas and the sample gas with aerosols. Sheath gas is to flow near the walls and act as a buffer layer keeping aerosols away from hitting inner surfaces. The sheath gas is assumed to be aerosol-free, but a future study will explore the effects of including the particles into the sheath gas flow mainly to quantify the deterioration of transmission efficiency in long time operations. The results suggest that the aerosol particles can be focused on a narrow beam and transferred into a differentially pumped module for further removal of the gas phase. Lighter gas molecules will undergo faster radial thermal expansion than heavier particles when subsequently transferred from high to low-pressure segments of the differentially pumped module. As a result, the heavier aerosol beam will retain its low divergence and remain confined axially. Effectively, the differential pumping module will act as an aerosol particle filter as it separates the much lighter gas phase from the heavier particles. This relative enrichment of aerosols will improve the sensitivity of the apparatus to sub ppb levels and ensure that *both pressures and gas flows are within the pumping capabilities* of Creare pumps. The purpose of the relaxation cell (see Fig.2) at the inlet of the NanoJet flow cell is to slow down the aerosol particles behind the piezoelectric valve²¹ and entrained them in the sheath gas flow. The sheath gas is recycled atmospheric gas from which particles are removed using the cyclone separator, and it provides a laminar gas flow to support the transfer of the aerosols within the relaxation cell. Particle-free sheath gas ensures near 100%

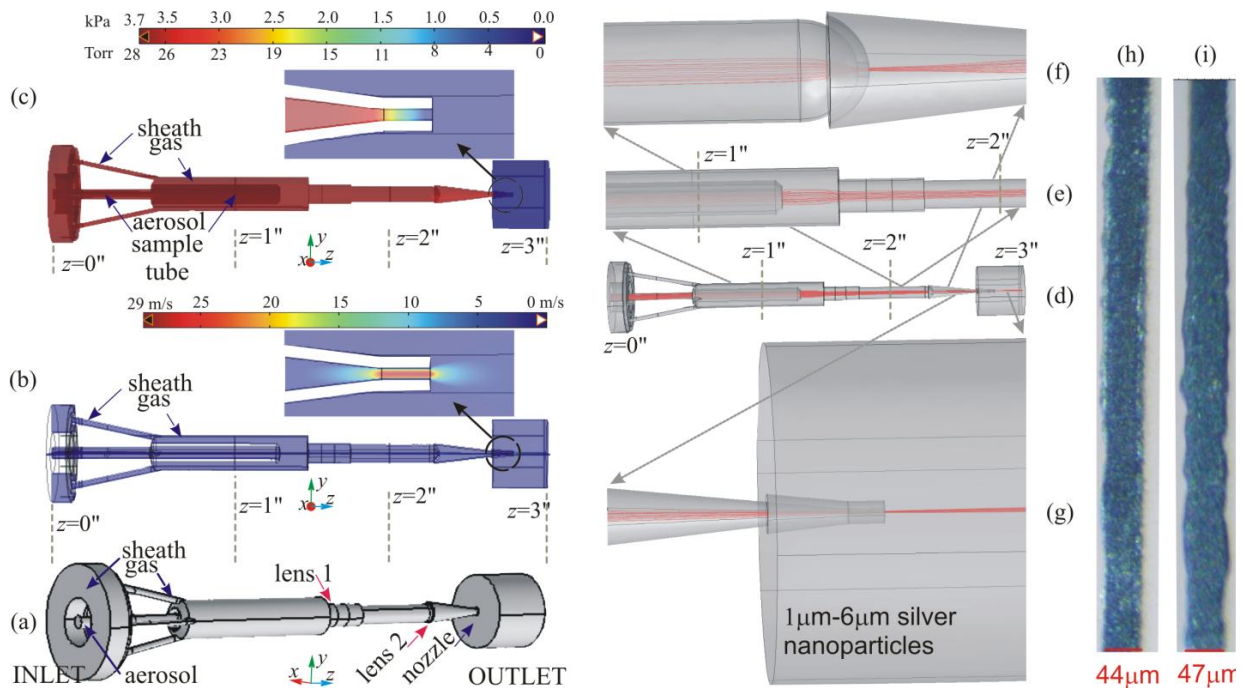


Figure 4: Summary of modeling¹⁷ (a-g) and experimental (h,i) results. (a) central tube brings aerosols into the sheath gas flow passing through the focusing assembly and the outlet nozzle. The axial distribution of carrier gas velocity (b) and pressure (c) fields supports near 100% transmission efficiency for 1-6 μm particles. Aerosols are initially released into the aerosol tube, and (d) their trajectories, here given as solid red curves, are traced along the flow cell's length. The enlarged sections of the flow cell correspond to the first (e) and the second (f) focusing lenses. The exit nozzle (g) is focusing 1 μm and 6 μm aerosols into the 60 μm and 40 μm wide particle beam, respectively. Modeling predictions are confirmed by electron microscope imaging of beam widths after 1min (h) and after 240min (i) of continuous operations.

transmission for particles in the $0.3\mu\text{m} - 7\mu\text{m}$ size range. In a future study, we will explore the possibility of using lower relaxation cell pressures P_{rx} (below 1 Torr) to reduce the gas load on the pumping system and extend the operation time.

After expansion through the NanoJet outlet nozzle, the atmosphere gas sample will drift radially away from the beam axis (cf. Fig.2). Thus, the sample gas will experience strong radial expansion and will be deflected out of the aerosol beam by skimmers and pumped out. Heavier particles will inertially remain constrained in the vicinity of the beam axis. Consequently, particles will experience negligible radial expansion and will freely pass through the first skimmer into the LOAC sensor, where they will be sized, counted, and characterized for their refraction index. If LOAC is not used, particles accompanied by negligible amounts of gas will be injected directly into the test high-vacuum chamber through the second skimmer. In this way, the NanoJet flow cell not only keeps focusing particles near the lens axis but also improves the aerosol abundance relative to the dominant gas component in the atmosphere.

B. Detailed Design and Performance

Figure 5 illustrates the entry TRL2 components of the apparatus that will reach TRL4 at the end of this project. The LOAC is TRL-6, but it is currently redesigned at TRL-2 by CNRS and CNES to be high-vacuum compatible at operating pressures below $1\text{E-}4\text{Torr}$. The IDS NanoJet flow cell in Fig. 5a is mounted to the LOAC's inlet but can easily be directly mounted on the 3D-printed vacuum chamber to eliminate dependency on the LOAC sensor. To prevent the adhesion of vaporized aerosols, which might lead to cross-contamination between sampling runs, the inner surface of the 3D-printed vacuum chamber is treated with a silicon-barrier coating (SilcoGuard by SilcoTek²²). Gans *et al.*²³ demonstrated that 3D-printed titanium is ultra-high vacuum compatible as-is without further surface finishing with an estimated maximum outgassing rate of $5.2\text{E-}11\text{ TorrL/cm}^2\text{s}$. The size of the aerosols measured by LOAC can be verified in an independent test by using two built-in virtual impactors placed at the exit of the NanoJet flow cell (see green shaded nozzle in the center of Fig 5b). Replaceable virtual impactors are not an integral part of the apparatus and are used only for size distribution calibrations in the laboratory set-up, and as such, a new set will be installed for each new calibration run. The IDS will carry out compressible flow modeling to develop an ultra-compact NanoJet aerosol focusing assembly for particle sizes $0.2 - 7\mu\text{m}$, which are expected to be present in the cabin atmosphere of the International Space Station (ISS).

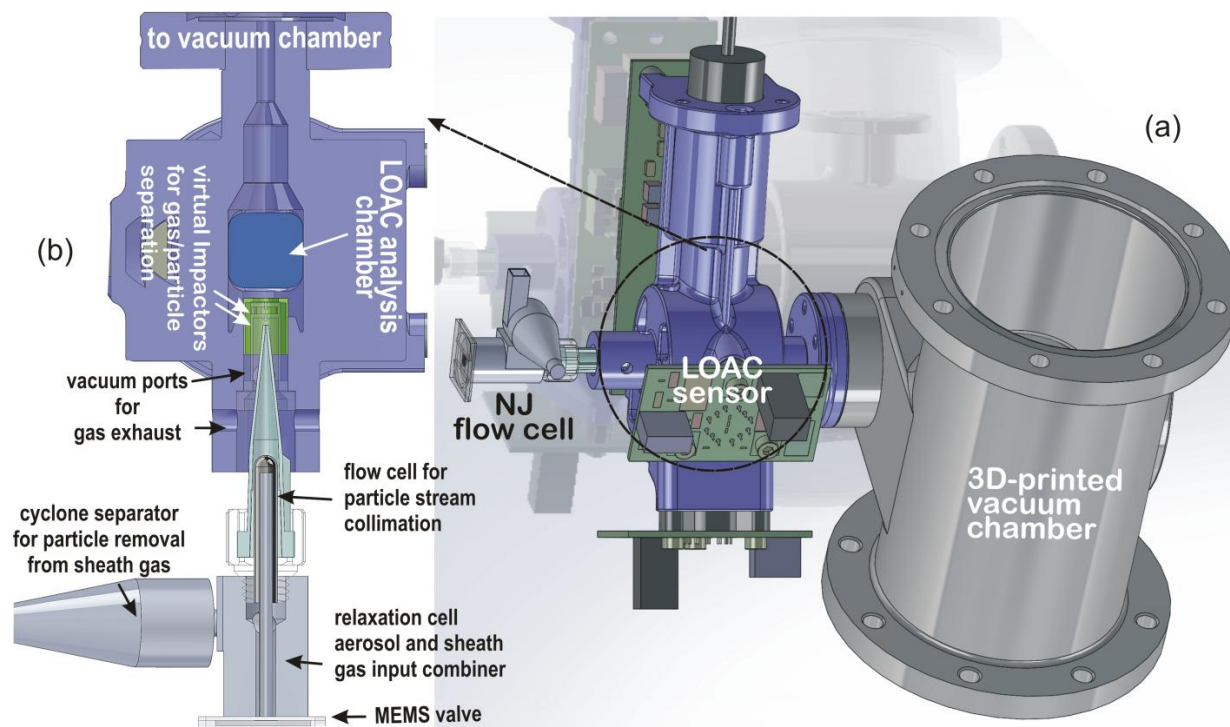


Figure 5: Entry TRL components. (a) Computer model of NanoJet flow cell (TRL-2) coupled with MEMS valve (TRL-4), cyclone separator (TRL-2), LOAC sensor (TRL-2), and 3D-printed non-corrosive vacuum chamber (TRL-2); (b) enlarged interface between NanoJet flow cell and LOAC sensor where each functional element is labeled.

The baseline experiments carried out over 4 hours of continuous operation are shown in Figs. 4h and 4i. The aerosol beam width was sampled at 1 min intervals, and results show no signs of a steady increase in width (a symptom of clogging). For these tests, silver nanoparticles were dispersed inside 2 μm commercial ink droplets (UTDots Ag40X). The diameters of focusing lenses inside the NanoJet flow cell were 750 μm and 150 μm for lens 1 and lens 2 (plastic, tapered). Figures 4h and 4i confirm that during 4 hours, the aerosol beam width remains within (46 ± 3) μm . It is important to note that the sheath gas is fed into the flow cell through separate gas flow channels to provide a coaxial gas feed that surrounds the aerosol-laden carrier gas as it passes through the flow cell. The aerosol and sheath gas flows are combined in the flow cell before the aerosol is passed through the first concentrating lens. The sheath gas constricts the aerosol stream diameter and prevents the aerosol from impacting on walls. This first focusing stage of the NJ flow cell relies largely on hydrodynamic focusing to constrict the aerosol stream diameter. In this case, the aerosol gas and sheath gas flows act as two fluid streams; the higher volumetric flow rate of the sheath gas is used to force the aerosols toward the flow cell's central axis. Once the sheath and aerosol gas streams are combined, the second orifice (see Fig. 4) in the flow path acts as an aerodynamic lens to further concentrate the aerosol stream by acting on sequentially smaller aerosol particles until the full range of particle sizes contained in the aerosol stream is fully collimated. The combination of hydrodynamic and aerodynamic focusing of the aerosol particles provides high transmission efficiency required for extended operation in the ISS cabin atmosphere.

IV. Laboratory characterization

Facilities at Caltech exist to characterize the piezoelectric valve and aerodynamic lens systems. Calibration aerosols in the submicron size regime will be produced by using a constant flow nebulizer²⁴. Present nebulizers in the Flagan laboratory are constructed from stainless steel; a Teflon version will be constructed for experiments using corrosive aerosols. The nebulizers produce a polydisperse aerosol that is roughly log-normally distributed with a geometric standard deviation of about 1.35. To produce a monodisperse aerosol, we will classify the generated polydisperse aerosol using a long cylindrical column differential mobility analyzer (DMA by TSI Inc.), which is based upon the original design of Knutson and Whitby²⁵. The aerosol is first charge-conditioned to produce a steady-state charge distribution in which most charged particles carry a single elementary charge. The particles are then classified by migrating from a small flow introduced near one electrode of the coaxial-cylinder DMA across a particle-free sheath flow. Those particles that reach the counter electrode at a downstream sample extraction port are extracted in a small, classified sample flow. Those classified particles, which range in size from about 20 nm to 860 nm for the flow conditions anticipated, can be controlled in size within about 10% on diameter for the larger sizes.

Calibration particles larger than about 5 μm diameter will be produced using a vibrating orifice aerosol generator²⁶ (VOAG). Indeed, monodisperse aerosols at intermediate sizes are difficult to produce. Monodisperse particles such as polystyrene latex (PSL) are commercially available as a stabilized suspension in a liquid. They are commonly used for calibration of aerosol instruments over a range of sizes, measuring from a few tens of nanometers to supermicron sizes. These aerosols, ranging from DMA to VOAG, will be used to characterize the aerodynamic lens system's quantitative performance. For characterization of the integrated measurement system, multistage virtual impactors can generate relatively narrow size distributions; the size distributions will be characterized using the scanning electrical mobility spectrometer²⁷ (SEMS, also known as the scanning mobility particle sizer, SMPS).

Calibration aerosols will be generated using existing systems operating at atmospheric pressure to produce a continuous flow of calibration particles. The number concentration of the calibration aerosol will be quantified by extracting a slip-stream of the calibration aerosol flow and counting with a condensation particle counter^{28,29} (CPC). Independent characterization of the LOAC sensor will be performed at atmospheric pressure to quantify its sizing capability and transmission efficiency. The calibrated LOAC will then be coupled to the NanoJet aerosol separator and the 3D-printed vacuum chamber equipped with an RGA mass detector to quantify the transmission efficiency of the adjustable MEMS piezoelectric valve.

A. Differentially pumped vacuum system

The JPL differentially pumped system (DPS, see Fig. 2) has dedicated ports for miniature flight-grade Creare turbo-molecular pumps (mTMP1-3) and miniature Creare scroll pump (mSP). The DPS will enclose all components of the aerosol separator in an easy to mount package to which optionally the LOAC sensor or the 3D-printed vacuum chamber can be attached. For this study, the DPS is coupled to a single laboratory size (80L/s) turbo-molecular pump via a gas line manifold (see thin red line in the upper right side of Fig. 2) with variable line

conductance that is matched to the pumping speed (10L/s) of each flight-grade Creare miniature pump. In this way, testing of the DPS will be fully independent of, but still compatible with the future acquisition of miniature pumps. The DPS will contain the interface between the piezoelectric valve and vacuum-ready MicroPirani pressure gauges to actively control the piezoelectric valve gap G based on measured pressure at the inlet of the aerodynamic lens. The MEMS piezo valve will have mounted guides for easy insertion and tight fit to the IDS NanoJet aerosol separator.

B. Optical sizing and counting of aerosol particles

This study must design titanium, corrosion resistant³⁰, 3D-printed vacuum chamber (see Fig. 6a) in which chemical compositions of aerosol particles will be measured by 200 amu RGA quadrupole mass filter, and high-vacuum will be maintained by the HiCube 80L/s turbo-molecular pump. For sizing the aerosol particles, one LOAC instrument (see Fig. 6c) from the MeteoModem Company will be modified to be vacuum compatible. The LOAC provides an independent and portable test for the size distribution transmitted through the IDS NanoJet aerosol separator. LOAC sensor is devised by Renard *et al.*⁴ as a light optical aerosol counter and sizer (cf. Fig. 6c) for ground-based and balloon measurements of the size distribution of atmospheric particles.

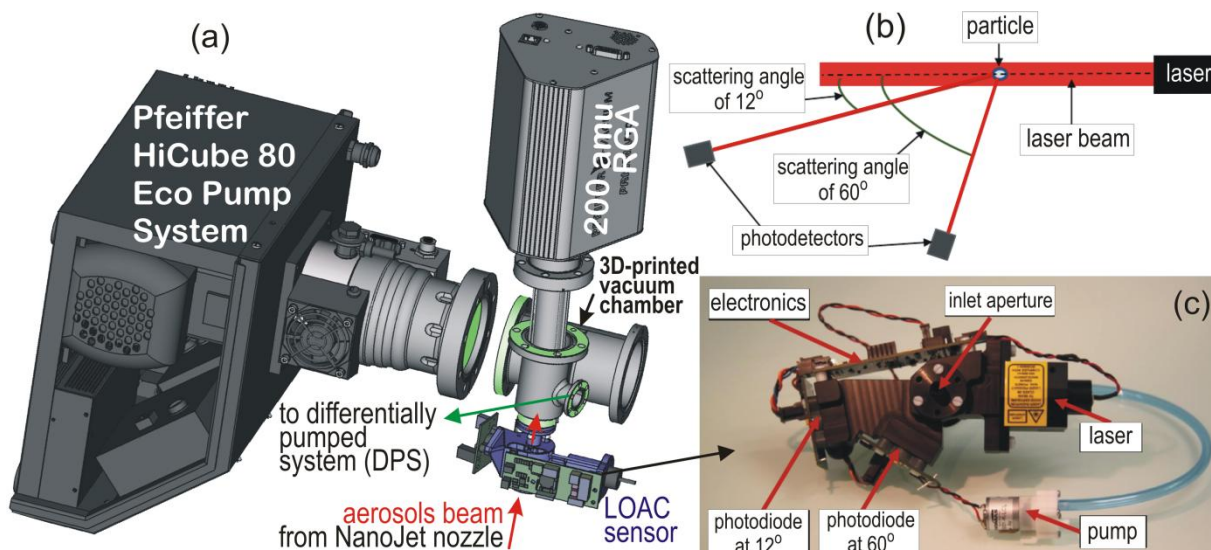


Figure 6: The LOAC instrument⁴: (a) CAD model of LOAC sensor mounted to the 3D-printed chamber; (b) principle of measurement; (c) picture of the sensor with the inlet aperture that will be attached to the NanoJet flow cell output nozzle, Fig. 5b.

The LOAC sensor will be mounted to the 3D-printed vacuum chamber (Fig. 6a) such that the aerosol beam entering the LOAC analysis chamber will cross a 650-nm ($\pm 5\%$), 25 mW laser beam (Fig. 6b). Two photodiodes record the scattered light at 11° – 16° and 55° – 65° angles. Light travels through glass windows to reach photodiodes providing fields of view of a few degrees. The electronic sampling had to be higher than 40 kHz, to resolve fast-moving particles because transit times of particles inside the laser beam are lower than 700 μs . The size calibration procedure is conducted by the 11° – 16° channel, which is almost insensitive to the refractive index of the particles. The 55° – 65° channel may be used as a comparison to the 11° – 16° channel measurements to determine the typology of the aerosol (carbonaceous particles, minerals, salts, or liquid droplets). The counting calibration provides us with total concentration measurements. The concentration uncertainty is $\pm 20\%$ for number densities above 100cm^{-3} whereas uncertainties in size calibration are $\pm 4\%$ for aerosols smaller than $0.6\ \mu\text{m}$, $\pm 5\%$ for aerosols in the 0.7 – $2\ \mu\text{m}$ range, and $\pm 10\%$ for aerosols greater than $2\ \mu\text{m}$.

C. Key performance metrics

Table 1 contains the key features of the proposed aerosol separator compared to other similar devices found in peer-reviewed literature and datasheets. Schreiner³¹ and Aerodyne³² lenses have been critically evaluated by Kamphus *et al.*³³. The performance of Enertechnix μADL lens³⁴ is adopted from publicly available 2009 datasheets.

Table 1: comparison of academic, commercial, military, and industrial aerodynamic lenses

Parameter	Schreiner lens	Aerodyne lens (inside AMS)	Enertechnix (μ ADL lens)	this study (IDS NanoJet lens)
outside pressure tolerance	43-760 Torr	\sim 760 Torr	\sim 760 Torr	1-75000 Torr
outlet pressure	<1 mTorr	< 10 mTorr	unpublished	< 1 μ Torr
length	107 mm	180 mm	40 mm	35 mm
# of orifices	7	5	2	2
orifice sizes	0.25-1.3mm	3-5mm	unpublished	0.15-0.7mm
variable aperture	no	no	no	yes
aerosol size range	300-3000 nm	80-800 nm	700- 5000 nm	200-7000 nm
transmission efficiency	$>90\%$	60-100%	50-100%	90-100%
concentration ratio	$\sim 1E6$	unpublished	unpublished	$\sim 1E8$
aerosol beam width	$>100\mu\text{m}$	unpublished	$>100 \mu\text{m}$	10-100 μm

V. Conclusion

The proposed aerosol separator will contribute to our capability to measure the composition of aerosol particles suspended in a wide variety of planetary, laboratory, industrial, and spacecraft cabin atmospheres using a variety of mass spectrometers. Its adaptive high-pressure tolerant piezoelectric aperture will open up chemical compositional studies of deep atmospheres previously deemed prohibitive due to overwhelming amounts of gas that need to be separated from the aerosol particles. More importantly, the adaptive aerosol separator will continue to operate at an optimal transmission rate despite changes in the outside pressure, simply by controlling the conductance of the piezoelectric aperture. To our knowledge, NASA does not have an instrument capable of yielding detailed molecular information from aerosol samples. The proposed instrument technology is both sensitive and quantitative and can measure aerosol distributions during atmospheric sampling by probes or landed. The chemical composition of aerosol particles can be obtained by coupling the proposed technology to mass spectroscopy-based instruments.

Acknowledgments

This study has been partially carried out at the Jet Propulsion Laboratory, California Institute of Technology, under the contract with the National Aeronautics and Space Administration. ©2020. California Institute of Technology. Government sponsorship acknowledged.

References

- ¹M. Essien, *Apparatuses and Methods for Stable Aerosol Deposition Using an Aerodynamic Lens System*, US20160193627A1 (2016).
- ²S. M. Madzunkov, D. Nikolić, *Accurate Xe Isotope Measurement Using JPL Ion Trap*, *J. Am. Soc. Mass Spectrom.* **25**(11), 1841-1852 (2014).
- ³D. Nikolić, S. M. Madzunkov, and M. R. Darrach, *Computer Modeling of an Ion Trap Mass Analyzer, Part I: Low-Pressure Regime*, *J. Am. Soc. Mass Spectrom.* **26**(12), 2115-2124 (2015).
- ⁴J.-B. Renard *et al.*, *LOAC: a light aerosols counter for ground-based and balloon measurements of the size distribution and the main nature of atmospheric particles, I. Principle of measurements and instrument evaluation*, *Atmos. Meas. Tech.*, **9**, 1721-1742 (2016).
- ⁵D. G. Nash, T. Baer, and M. V. Johnston, *Aerosol mass spectrometry: An introductory review*, *International Journal of Mass Spectrometry* **258**(1-3), 2-12 (2006).
- ⁶D. Keicher, M. Essien, J. Lavin, S. Whetten, S. Mani, *Next Generation Aerosol-Based Printing for Production-Level Printed Electronics*, *Flexible Electronics - Accelerating to Manufacturing (2017 FLEX)*, June 19-22 Monterey, California, USA (2017).
- ⁷R. Kline-Schoder, President & Principal Engineer of Creare, *Private Communication* (2018).
- ⁸P. Sorensen, R. Kline-Schoder, and R. Farley, *Wide Range Vacuum Pumps for the SAM Instrument on the MSL Curiosity Rover*, The 42nd Aerospace Mechanism Symposium, 463-470 (2014); Report Number NASA/CP-2014-217519, GSFC-E-DAA-TN14675
- ⁹F. Goesmann *et al.*, *The Mars Organic Molecule Analyzer (MOMA) Instrument: Characterization of Organic Material in Martian Sediments*, *Astrobiology* **17** (6-7), 655-685 (2017).
- ¹⁰P. R. Mahaffy *et al.*, *The Sample Analysis at Mars Investigation and Instrument Suite*, *Space Science Reviews* **170** (1-4), 401-478 (2012).

- ¹¹ MKS, *Series 905 MicroPirani Sensor Kit*, https://www.mksinst.com/mam/celum/celum_assets/resources/905DS.pdf
- ¹² K. Pant, C. T. Crowe, and P. Irving, On the design of miniature cyclones for the collection of bioaerosols, *Powder Technology* **125**, 260-265 (2002).
- ¹³ M. Griener et al., *Fast piezoelectric valve offering controlled gas injection in magnetically confined fusion plasmas for diagnostic and fuelling purposes*, *Review of Scientific Instruments* **88**, 033509 (2017).
- ¹⁴ M E.-H. Yang, C. Lee, J. Mueller, and T. George, *Leak-Tight Piezoelectric Microvalve for High-Pressure Gas Micropropulsion*, *J. Microelectromechanical Systems* **13**(5), 799-807 (2004).
- ¹⁵ J. Simcic, J.C. Lee, S. Madzunkov, D. Nikolić, A. Belousov, *Piezo-Electric Inlet System for Atmospheric Descent Probe*, 16th International Planetary Probe Workshop & Short Course titled Ice Giants: Exciting Targets for Solar System Entry Probes Exploration, 6–7 July 2019 Oxford University.
- ¹⁶ ANSYS Inc., *ANSYS Fluent Theory Guide, Release 18.2*, 275 Technology Drive, Canonsburg, PA 15317, November 2018.
- ¹⁷ D. Nikolić, D. Keicher, and F.-G. Fan, *Design of an Aerodynamic Lens for PM2.5 Chemical Composition Analysis*, 49th International Conference on Environmental Systems, 07-11 July 2019 Boston, Massachusetts, USA, ICES_2019_366 (2019).
- ¹⁸ D. Nikolić, J. Simcic, and S. Madzunkov, *Expected Performance of the QIT-MS Mass Spectrometer in Venus' Atmosphere*, 17th Meeting of the Venus Exploration and Analysis Group (VEXAG), November 6-8, 2019 in Boulder, Colorado USA, LPI Contribution No. 2193, id.8024 (2019).
- ¹⁹ K.H. Baines, J.A. Cutts, D. Nikolić, S.M. Madzunkov, J.-B. Renard, O. Mousis, L.M. Barge, and S.S. Limaye, *An Aerosol Instrument Package for Analyzing Venusian Cloud Particles*, 17th Meeting of the Venus Exploration and Analysis Group (VEXAG), November 6-8, 2019 in Boulder, Colorado USA, LPI Contribution No. 2193, id.8010 (2019).
- ²⁰ K.H. Baines, J.A. Cutts, D. Nikolić, S.M. Madzunkov, M.L. Delitsky, S.S. Limaye, K. McGouldrick, *The JPL Venus Aerosol Mass Spectrometer Concept*, 16th International Planetary Probe Workshop & Short Course titled Ice Giants: Exciting Targets for Solar System Entry Probes Exploration, 6–7 July 2019 Oxford University.
- ²¹ X. Wang and P. H. McMurry, *A Design Tool for Aerodynamic Lens Systems*, *Aerosol Sci. Tech.* **40**, 320-334 (2006).
- ²² SilcoTek. URL: <https://www.silcotek.com/silcod-technologies/silcoguard-high-purity-coating>
- ²³ A. R. Gans, M. M. Jobbins, D. Y. Lee, and S. A. Kandel, *Vacuum compatibility of silver and titanium parts made using three-dimensional printing*, *Journal of Vacuum Science and Technology A* **32**, 023201 (2014).
- ²⁴ B.Y.H. Liu and K. W. Lee, *An aerosol generator of high stability*, *American Industrial Hygiene Association Journal*, **36**(12), 861-865 (1975).
- ²⁵ E.O. Knutson and K.T. Whitby, *Aerosol classification by electric mobility: apparatus, theory, and applications*, *Journal of Aerosol Science* **6**(6), 443-451 (1975).
- ²⁶ R. N. Berglund and B.Y.H. Liu, *Generation of monodisperse aerosol standards*, *Environ. Sci. Technol.* **7**(2), 147-153 (1973).
- ²⁷ S.C. Wang and R.C. Flagan, *Scanning Electrical Mobility Spectrometer*, *Aerosol Science and Technology* **13**(2), 230-240 (1990).
- ²⁸ D. Sinclair and G.S. Hoopes, *A Continuous Flow Condensation Nucleus Counter*, *Journal of Aerosol Science* **6**(1), 1-7 (1975).
- ²⁹ P.H. McMurry, *The History of Condensation Nucleus Counters*, *Aerosol Science and Technology* **33**(4), 297-322 (2000).
- ³⁰ TIMET, *Corrosion Resistance of Titanium*, U.S. Nuclear Regulatory Commission Report ML993210187 (1999); <https://www.nrc.gov/docs/ML9932/ML993210187.pdf>.
- ³¹ J. Schreiner et al., *Focusing of Aerosols into a Particle Beam at Pressures from 10 to 150 Torr*, *Aerosol Sci. Technol.* **31**, 373-382 (1999).
- ³² P.S.K. Liu et al., *Transmission Efficiency of an Aerodynamic Focusing Lens System: Comparison of Model Calculations and Laboratory Measurements for the Aerodyne Aerosol Mass Spectrometer*, *Aerosol Science and Technology* **41**(8), 721-733 (2007).
- ³³ M. Kamphus et al., *Comparison of Two Aerodynamic Lenses as an Inlet for a Single Particle Laser Ablation Mass Spectrometer*, *Aerosol Science and Technology* **42**(11), 970-980 (2008).
- ³⁴ Enertech, *Aerodynamic lens: advanced concentration technology for superior sensitivity and detection* (2010); *Advanced aerosol technology: sampling, concentration, collection, delivery and detection* (2009).